JOURNAL OF NANO- AND ELECTRONIC PHYSICS
Vol. **10** No 2, 02036(5pp) (2018)

ЖУРНАЛ НАНО- ТА ЕЛЕКТРОННОЇ ФІЗИКИ
Том **10** № 2, 02036(5cc) (2018)

Properties of Undoped and (Al, In) Doped ZnO Thin Films Prepared by Ultrasonic Spray Pyrolysis for Solar Cell Applications

A. Djelloul[1,2,*], Y. Larbah[3], M. Adnane[1], B. Labdelli[2], M.I. Ziane[2], A. Manseri[2], A. Messaoud[2]

[1] *Département de Technologie des Matériaux, Faculté de Physique, Université des Sciences et de la Technologie d'Oran Mohamed Boudiaf USTO-MB, BP 1505, El M'naouer, 31000 Oran Algérie*
[2] *Centre de Recherche en Technologie des Semi-Conducteurs pour l'Energétique 'CRTSE', 02 Bd Frantz Fanon, BP 140, 7 Merveilles, Alger, Algérie*
[3] *Spectrometry Department, Nuclear Technical Division, Nuclear Research Center of Algiers, 2 Bd., Frantz Fanon, BP 399, Algiers 16000, Algeria*

(Received 26 December 2017; revised manuscript received 28 April 2018; published online 29 April 2018)

Zinc oxide (ZnO) is an *n*-type semiconductor with a large optical gap (3.4 eV) belonging to the transparent conductive oxides family (TCO). Strongly present as optical window in the chalcopyrite based structures CIGS and CIS.

The structural, morphological, optical and electrical properties of ZnO thin films deposited onto glass substrates by ultrasonic spray pyrolysis (USP) technique have been investigated. For comparison and a better understanding of physical properties of undoped and (Al, In) doped ZnO thin films, a number of techniques, including XRD, SEM, optical absorption method (UV) and four-point probe technique were used to characterize the obtained ZnO thin films. Structural analysis shows that all the films were found to be polycrystalline with a wurtzite structure and show a (1 0 1) preferential growth. Besides, we noted that the preferred orientation does not depend on the nature of dopant. The band gaps (E_g) varied from 3.35 to 3.37 eV by Al and In dopants.

Keywords: Zinc oxide, Al doped ZnO, In doped ZnO, Ultrasonic Spray Pyrolysis.

DOI: 10.21272/jnep.10(2).02036 PACS numbers: 68.55. – a, 73.50. – h, 81.15.Cd, 81.15.Rs

1. INTRODUCTION

Zinc oxide (ZnO) is one of the most multifunctional semiconductor material used in different applications' domains like optoelectronic devices [1], light emitting diode (LED) [2], gas sensors [3], and photovoltaic devices [4], owing to its direct wide band gap of 3.37 eV [5], n-type conductivity and high exciton binding energy of 60 meV [6]. On the other hand, it is one of the most potential materials for being used as a TCO (Transparent Conducting Oxides) because of its high electrical conductivity due to lack of oxidation and high transparency in the visible wavelength range. This property can be improved by a selective doping substituting Zn with various metals such as indium (In) [7], aluminium (Al) [8] and gallium (Ga) [9]. ZnO (doped and undoped) is currently used in the CIGS thin-film solar cell [10].

Several deposition techniques have been used for the growth including, magnetic sputterig [11], laser deposition [12], sol-gel [13] and spray pyrolysis [14].

In the present work, undoped and (Al, In) doped ZnO thin films were prepared by ultrasonic spray pyrolysis [15] onto glass substrate at temperature of 400°C.

This technique is attractive and widely used, because it is an inexpensive, simple, without toxicity and non-contaminating production process. ZnO can be doped with a wide variety of ions. The ZnO doping is achieved by replacing Zn^{2+} atoms of elements of higher valance such as In^{3+}, Al^{3+}, Sn^{4+} and Pb^{4+} [16]. The structural, morphological, optical and electrical characterization of undoped and doped ZnO films were evaluated. Such as better stoichiometry control, better homogeneity, low processing temperature, lower cost, easier fabrication of large area films, and having an easy coating process of large substrates.

2. EXPERIMENTAL DETAILS

2.1 Preparation of Thin Film

Films were deposited on glass substrates thickness (1.35 mm) and size (75 × 25 mm^2), these substrates were ultrasonically cleaned with acetone, methanol (for 30 minutes) and finally washed by deionized water, in order to clean them.

A spray ultrasonic technique was used to obtain undoped and (Al, In) doped zinc oxide thin films. The starting solution used for the films investigated here is composed with 0.1 M of zinc acetate dihydrate ($C_4H_6O_4Zn.2H_2O$). Doping sources were indium (III) chloride ($InCl_3$), and aluminum (III) chloride hydrated, ($AlCl_3$, $6H_2O$). Both, the precursor and the dopant source (with the doping ratio In/Zn, Al/Zn were fixed at 5 %) were dissolved in methanol alcohol.

The deposition substrates temperature was fixed equal to 400 °C, the distance between the substrate and the spray gun nozzle was fixed at 20 cm. The deposition time was fixed at 5min for all samples. The selected optimal temperature of the substrates is 400 °C because the deposited layers have the lowest sheet resistance and good transparency. After depositing the film, it was allowed to cool to room temperature. A

* djelloulcrtse@gmail.com

schematic drawn of the spray pyrolysis apparatus for the synthesis of the undoped and (Al, In) doped ZnO thin films is depicted in Fig. 1.

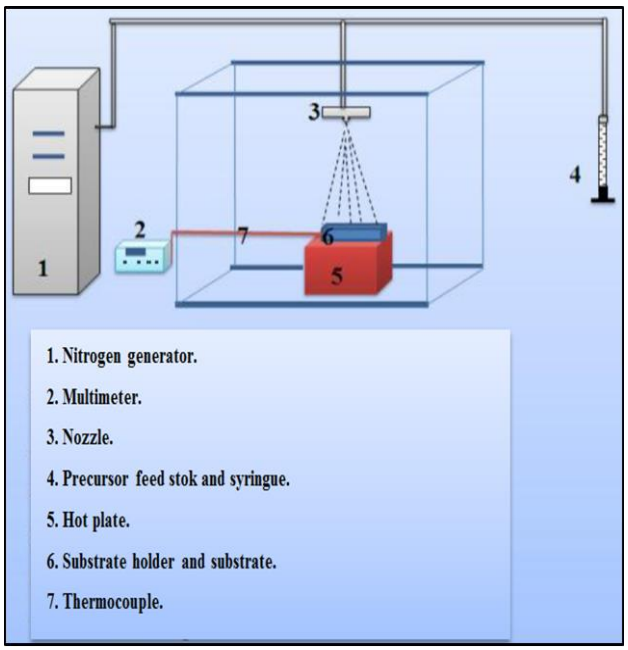

Fig. 1 – Schematic diagram of spray pyrolysis process of ZnO and (Al, In) doped ZnO thin films preparation

The structural, morphological, optical and electrical analysis of films has been investigated by XRD, SEM, UV spectroscopy and four-point probe technique were used to characterize the obtained ZnO thin films.

The substrate temperature was monitored with a thermocouple and controlled electronically. The thickness of the films was determined by ellipsometry using SEMILAB Spectroscopic Ellipsometter. X-ray measurements were done by the PANalytical X'PERT Pro Philips diffractometer with a CuKα radiation (λ = 1.54059 Å). The morphology of samples was observed by scanning electronic microscope (SEM) Philips SEM505 (HT/15kV). The optical transmittance measurements have been carried out with a spectrophotometer (Cary 500) in the wavelength range (300-1200) nm. Finally, the electrical properties (sheet resistance and resistivity) of the films were measured using the four-point probe conventional instrument. Therefore the samples were referenced IZO for In doped ZnO and AZO for Al doped ZnO.

3. RESULTS AND DISCUSSION

3.1 Structural Properties

The XRD data was used to investigate the structural properties before and after incorporation of (In, Al) in the ZnO thin films. The comparison of spectra with the (JBSD 36-1451) specifications ZnO confirmed that we have only the peaks of ZnO phase in the XRD spectrum. This can be the result of doping the crystalline ZnO or of amorphous phase formation.

Figure 2 shows the recorded XRD patterns in the prepared ZnO thin films. As can be seen from figure 2, this patterns are composed with several diffraction peaks assigned to (100), (002), (101), (102), (110) and (103) planes where the strongest one is (101).

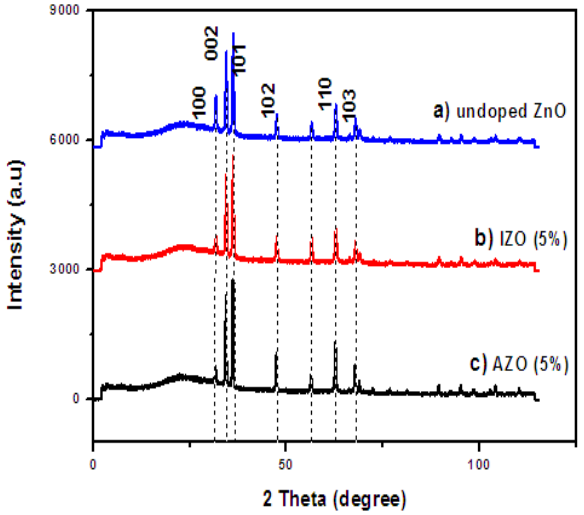

Fig. 2 – Spectra of X-ray diffraction of: (a) undoped ZnO, (b) ZnO doped 5 wt % In (IZO) and (c) ZnO doped 5 wt % Al (AZO), thin films

This suggests that all the elaborated films are polycrystalline in nature and have a hexagonal wurtzite structure with preferred orientation along the (101) plane [17]. Aluminum doping causes the peaks (102), (110) and (103) to emerge [Figure 2(c)], whereas indium doping causes its intensity to decrease [Figure 2(b)]; this result is in agreement with reference [18].

The lattice spacing was calculated using the Bragg's formula [19]:

$$2d_{hkl}\sin\theta = n\lambda \quad (1)$$

where (h k l) are Miller indices; d_{hkl} is the lattice spacing; θ is half of Bragg angle; and λ is the wavelength of the target XRD.

The lattice parameters (a, c) were calculated using the following equation [20]:

$$\frac{1}{d_{hkl}^2} = \frac{4}{3}\left[\frac{h^2+hk+k^2}{a^2}\right] + \frac{l^2}{c^2} \quad (2)$$

The grain size (D) of undoped and (Al, In) doped ZnO thin films were evaluated to be between 12 nm to 15 nm by using the Debye Scherrer's formula [21].

$$D = \frac{K.\lambda}{\beta\cos\theta} \quad (3)$$

Where β is the full width at half maximum (FWHM) of the diffraction peak;

The grain size (D) values calculated for the $2\theta = 36.25^{o}$ are ZnO = 15 nm, IZO = 13 nm and AZO = 12 nm. By including the indium and aluminum ions in the ZnO lattice the crystal order is decreased.

The AZO films grow mainly oriented in the [101] direction, this result was found by Benhaliliba et al [22]. Aluminum doping induced a decrease in average grain size. Many authors have reported that Al doping decrease the grain size due to the substitution of Zn ions (Rionic = 0.074 nm) by the Al ion (Rionic = 0.054 nm) and the difference between them [23].

The lattice parameters (a and c) and grain size in the direction (101) are sensitive to the nature of the

Table 1 – Specific parameters of undoped and doped ZnO thin films deposited on glass substrate at 400 °C

Samples	a (Å)	c (Å)	c/a (Å)	D (nm)
ZnO	3.249	5.210	1.603	15
AZO	3.243	5.195	1.602	12
IZO	3.240	5.187	1.601	13
JCPDS 36-1451	3.242	5.194	1.602	-

doping (Table 1). This result is in agreement with Merike Kriisa et al. [24]. The values for doped films are smaller than for undoped films. This can be attributed to microdeformations produced by residual stresses [25]. Calculated values for lattice parameters are in good agreement with JCPDS data. The ratio value c/a for the AZO layer is identical to the standard value (JCPDS). Thus, aluminum doping improves the crystalline quality.

3.2 Morphological Properties

The morphology of the surface of our layers was analyzed by SEM microscopy (Secondary Electron Microscope). Figure 3 shows the SEM images of the undoped ZnO, IZO and AZO thin films deposited on glass at 400 °C. The SEM images (Fig. 3) show that the deposited ZnO films are continuous, dense and distributed over the entire area with a rough surface.

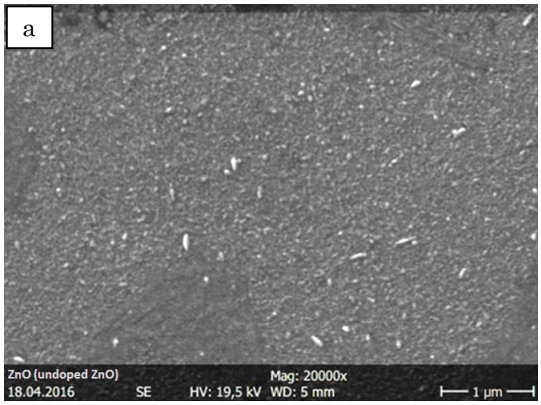

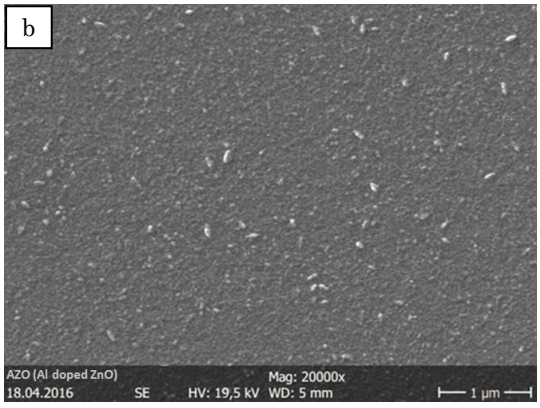

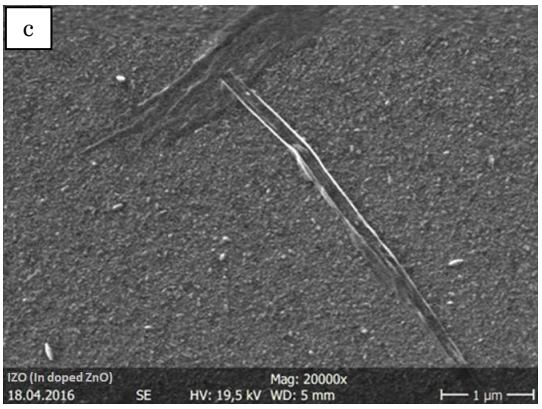

Fig. 3 – Surface SEM micrographs for (a) ZnO, (b) AZO and (c) IZO films deposited on glass substrate at 400 °C

The results of the structural analyzes are confirmed by the SEM images (Fig. 3) which show a granular and polycrystalline morphology with a smooth surface of low roughness due to the small thickness of the deposited layers with small rounded grains d an average diameter varying between 5 and 50 nm. From these images, it is clear that the ZnO, IZO and AZO layers have small uniform size grains in the form of nanoparticles. However, the grain size as measured from the surface images is higher than the values calculated from the X-ray diffraction measurements, indicating that these grains are probably an aggregate of crystallites.

3.3 Optical Properties

The optical properties of undoped ZnO, IZO and AZO thin films were investigated by means of optical transmission in the range (300-1200 nm) using a spectro- photometer. The transmittance spectra of these films are shown in Fig. 4.

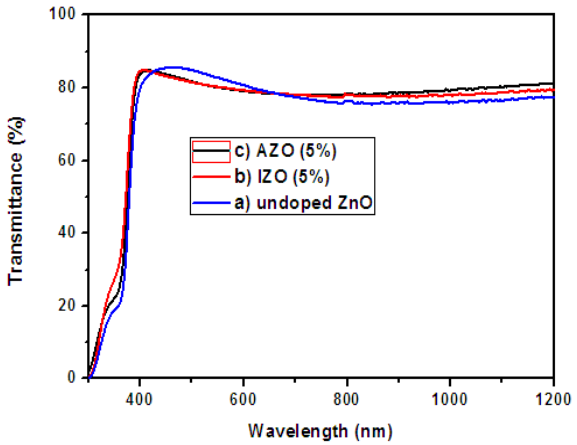

Fig. 4 – Transmittance spectra of: a) undoped ZnO, b) In-doped ZnO and c) Al-doped ZnO thin films deposited onto glass substrate

The transmission of the doped films is found to be superior to the undoped film. A maximum transmittance of 85 % is obtained for undoped ZnO films at around 600 nm, whereas both the IZO and AZO films exhibit a maximum of 80 % at the same wavelength. The energy gap (E_g) of the ZnO films can be calculated by using the relation [26]:

$$(\alpha hv)^2 = K(hv - E_g) \quad (4)$$

where «*K*» is a constant, «*h*» is Planck's constant and E_g is the band gap energy. The absorption coefficient (α) which is a function of the photon energy (hv) is calculated from the optical transmittance spectra results using the following equation [27]:

$$\alpha = \frac{-\ln(T)}{d} \quad (5)$$

where «*d*» is the thickness of the film and «α» is the absorption coefficient which is obtained from transmittance «*T*».

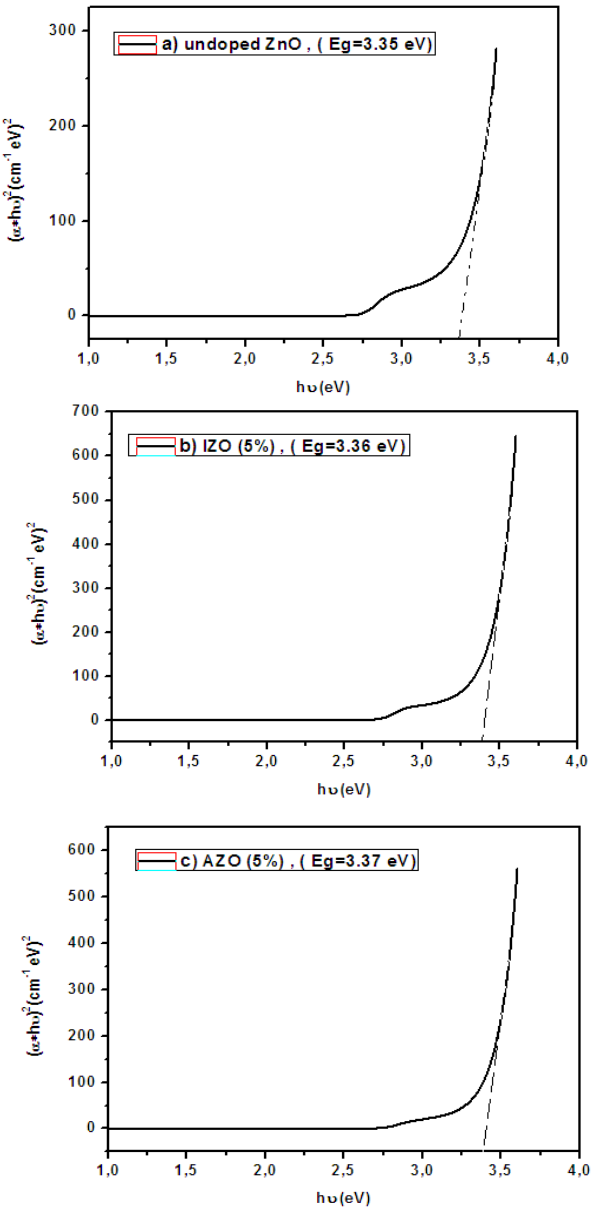

Fig. 4 – The optical energy gap of undoped and (Al, In) doped ZnO thin films: a) undoped ZnO, b) In-doped ZnO and c) Al-doped ZnO thin films

Figure 5 shows how the direct energy gap of the same coatings mentioned previously has been estimated by extrapolating the linear part of $(\alpha hv)^2$ plot versus photon energy (hv) to the wavelength axis. The optical band gaps of the ZnO, IZO and AZO samples are almost constant proving no structural modifications. ZnO film band gap is found to be 3.35 eV, the decrease of E_g is estimated at 0.01 and 0.02 respectively with In and Al doping. Similar effect has been observed for undoped and doped ZnO films grown by RF magnetron sputtering [28].

The wide direct band gap makes these films good material for potential applications in solar cell due to decreases the window absorption loses and that will improve the short circuit current of the cell.

3.4 Electrical Properties

The variations of the film thickness (d), resistivity (ρ), transmittance (T), refractive index (n_s) and energy band gap (E_g) for undoped and doped ZnO thin films are presented in Table 2.

Table 2 – XRD patterns analysis: Lattice parameters (a and c) and Grain size (D) in the direction (101)

Samples	d [nm]	ρ [Ωcm]	T [%]	n_s	E_g [eV]
ZnO	128	$1.50\ 10^{-3}$	80	2.08	3.35
IZO	117	$0.53\ 10^{-3}$	85	2.06	3.36
AZO	115	$0.63\ 10^{-3}$	85	2.06	3.37

The electrical properties (sheet resistance and resistivity) of the undoped and doped ZnO films are measured at room temperature by the four-point technique. The nature of the charge carriers were measured by the hot probe method. ZnO exhibits *n*-type conductivity. The films thickness and the refractive index were determined from the ellipsometric measurements. As can be seen, the thickness values are different and depend on nature of the dopant. This is due to the variation in the involved reactions during growth with the same doping ratio but with different precursors. The optical transmittance spectra for all undoped and doped ZnO films show a very good transmittance over the visible region, between 80 and 85 %. The optical band gaps of the films were determined to be approximately same values. The Eg values confirm the dopants' contribuition ZnO in the thin film. The thickness increase might be attributed to the dopants that increase the crystallisation nuclei concentration [29]. The Al-dopant might introduce secondary amorphous phase in the film network, which may also cause a decrease in the band gap energy. It was seen that the resistivity decrease with the doping sources.

4. CONCLUSION

In conclusion, undoped and (Al, In) doped ZnO thin films have been grown on glass substrate at 400 °C by the USP technique using zinc acetate dehydrate and doping sources (Al, In) were dissolved in methanol and deionized water.

Effect of In and Al dopants on the physical properties of ZnO thin films have been investigated. X-ray diffraction studies confirm that the films have polycrystalline nature with preferred orientation along the

(101) plane. The grain size values of the films are found to be 15, 13 and 12 nm for ZnO IZO and AZO thin films, respectively. The structural parameters (thicknesses, lattice parameters and grain size) of the films were determined. These parameters changed with In and Al dopants. XRD indicates that the cristallinity enhance with the indium doping, but the average crystallite grain size decrease with the aluminium doping. The SEM results indicates that all films are continuous, dense and distributed over the entire area with a rough surface. The optical transmittance spectra for all undoped and doped ZnO films show a very good transmittance over the visible region, between 80 and 85 %. The optical band gaps of the films were determined to be approximately same values. ZnO exhibits n-type conductivity. It was seen that the resistivity decrease with the Al and In doping sources.

These results indicate that, AZO and IZO films were synthesized by low cost way via USP method can be considered as the promising candidate for solar cell applications.

ACKNOWLEDGMENTS

This work was supported by all members of Laboratory of Electron Microscopy and Materials Sciences, University of Science and Technology of Oran 'USTO' and Centre de Recherche en Technologie des Semi-Conducteurs pour l'Energétique 'CRTSE', Algeria. The authors would like to thank the Algerian Ministry of Higher Education and Scientific Research and Directorate General for Scientific Research and Technological Development.

REFERENCES

1. A.B. Djurisic, A.M.C. Ng, X.Y. Chen, *Prog. Quantum Electron.* **34**, 191 (2010).
2. F. Chouikh, Y. Beggah, H. Mati, Y. Bouznit, M. Birem, N. Ariche, *Int. J. Nanoparticles* **6** No 23, 178 (2013).
3. Y. Bakha, K.M. Bendimerad, S. Hamzaoui, *Eur. Phys. J.* **55**, 30103 (2011).
4. S.C. Chuen, C. Feng-Cheng, D. Yi-Geng, W. Ping, *Sol. Energ.* **86**, 1435 (2012).
5. A. Zawadzka, P. Płociennik, J. Strzelecki, *Opt. Quant. Electron.* **46**, 87 (2014).
6. J.M. Myoung, W.H. Yoon, D.H. Lee, L. Yun, S.H. Bae, S.Y. Lee, *Jpn. J. Appl. Phys.* **41**, 28 (2002).
7. K. Won Mok, K. Dae Youg, L. In-Kyu, S. Yong Moon, C. Byung-Kim, L. Teak Sung, K. In-Ho, L. Kyeong Seok, *Thin Solid Films* **473**, 315 (2005).
8. K. Prabakar, K. Choongo, L. Chongmu, *Cryst. Res. Technol.* **40**, 1150 (2003).
9. N.F. Habubi, S.S. Chiad, S. Jabbar, W. Jabbar, *J. Arkansas Academy Sci.* **66**, (2012).
10. A. Romeo, M. Terheggen, D. Abou-Ras, D.L.Batzner, F.J. Haug, M. Kalin, D. Rudmann, A.N. Tiwari, *Prog. Photovoltaic: Res. Appl.* **12**, 93 (2004).
11. M. Bouderbala, S. Hamzaoui, B. Amrani, Ali H. Reshak, M. Adnane, T. Sahraoui, M. Zerdali, *Physica B* **403**, 3326 (2008).
12. G. Kaur, A. Mitra, K.L. Yadav, *Prog. Nat. Sci.: Mater. Int.* **25**, 12 (2015).
13. M.N. Kamalasanan, S. Chandra, *Thin Solid Films* **288**, 112 (1996).
14. Y. Larbah, M. Adnane, T. Sahraoui, *Mater. Sci.-Poland* **33**, 491 (2015).
15. S. Sali, M. Boumaour, S. Kermadi, A. Keffous, M. Kechouane, *Superlattice. Microstructure.* **52**, 438 (2012).
16. S. Roguai, A. Djelloul, Corinne Nouveau, T. Souier, A.A. Dakhel, M. Bououdina, *J. Alloy. Compd.* **599**, 150 (2014).
17. F. Bourfaa, M.L. Zeggar, A. Adjimi, M.S. Aida, N. Attaf. *IOP Conf. Series: Mater. Sci. Eng.* **108**, 012049 (2016).
18. K.A. Salman, K. Omar, Z. Hassan, *Mater. Lett.* **68**, 51 (2012).
19. C. Zegadi, A. Abderrahmane, A. Djelloul, S. Hamzaoui, M. Adnane, D. Chaumont, K. Abdelkebir, *Int. Rev. Phys.* **9** (2015).
20. T. Prasada Rao, M.C. Santhoshkumar, *Appl. Surf. Sci.* **255**, 4579 (2009).
21. A. Djelloul, M. Adnane, Y. Larbah, T. Sahraoui, C. Zegadi, A. Maha, B. Rahal, *J. Nano- Electron. Phys.* **7** No 4, 04045 (2015).
22. M. Benhaliliba, C.E. Benouis, M.S. Aida, F. Yakuphanoglu, A. Sanchez Juarez, *J. Sol-Gel. Sci. Technol.* **55**, 335 (2010).
23. S.D. Shinde, A.V. Deshmukh, S.K. Date, V.G. Sathe, K.P. Adhi, *Thin Solid Films* **520**, 1212 (2011).
24. M. Kriisa, M. Krunks, E. Kärber, M. Kukk, V. Mikli, A. Mere, *J. Nanomaterials* **2013**, 423632 (2013).
25. C.E. Benouis, M. Benhaliliba, A. Sanchez Juarez, M.S. Aida, F. Chami, F. Yakuphanoglu, *J. Alloy. Compd.* **490**, 62 (2010).
26. A. Djelloul, M. Adnane, Y. Larbah, M. Zerdali, C. Zegadi, A. Messaoud, *J. Nano- Electron. Phys.* **8** No 2, 02005 (2016).
27. A. Djelloul, M. Adnane, Y. Larbah, S. Hamzaoui, *J. Opt. Adv. Mater.* **18**, No 1-2, 136 (2016).
28. C. Lung, M. Toma, M. Pop, D. Marconi, A. Pop, *J. Alloy. Compd.* **725**, 1238 (2017).
29. M.A. Mahadik, Y.M. Hunge, S.S. Shinde, K.Y. Rajpure, C.H. Bhosale, *J. Semiconductors* **36**, 033002 (2015).